

## Ultra-low noise TES bolometer arrays for SAFARI instrument on SPICA

Khosropanah, P.; Suzuki, T.; Ridder, M. L.; Hijmering, R. A.; Akamatsu, H.; Gottardi, L.; Van Der Kuur, J.; Gao, J. R.; Jackson, B. D.

**DOI**

[10.1117/12.2233472](https://doi.org/10.1117/12.2233472)

**Publication date**

2016

**Document Version**

Final published version

**Published in**

Proceedings of SPIE

**Citation (APA)**

Khosropanah, P., Suzuki, T., Ridder, M. L., Hijmering, R. A., Akamatsu, H., Gottardi, L., Van Der Kuur, J., Gao, J. R., & Jackson, B. D. (2016). Ultra-low noise TES bolometer arrays for SAFARI instrument on SPICA. In *Proceedings of SPIE: Millimeter, Submillimeter, and Far-Infrared Detectors and Instrumentation for Astronomy VIII* (Vol. 9914). Article 99140B SPIE. <https://doi.org/10.1117/12.2233472>

**Important note**

To cite this publication, please use the final published version (if applicable).  
Please check the document version above.

**Copyright**

Other than for strictly personal use, it is not permitted to download, forward or distribute the text or part of it, without the consent of the author(s) and/or copyright holder(s), unless the work is under an open content license such as Creative Commons.

**Takedown policy**

Please contact us and provide details if you believe this document breaches copyrights.  
We will remove access to the work immediately and investigate your claim.

# PROCEEDINGS OF SPIE

[SPIDigitalLibrary.org/conference-proceedings-of-spie](https://spiedigitallibrary.org/conference-proceedings-of-spie)

## Ultra-low noise TES bolometer arrays for SAFARI instrument on SPICA

P. Khosropanah, T. Suzuki, M. L. Ridder, R. A. Hijmering, H. Akamatsu, et al.

P. Khosropanah, T. Suzuki, M. L. Ridder, R. A. Hijmering, H. Akamatsu, L. Gottardi, J. van der Kuur, J. R. Gao, B. D. Jackson, "Ultra-low noise TES bolometer arrays for SAFARI instrument on SPICA," Proc. SPIE 9914, Millimeter, Submillimeter, and Far-Infrared Detectors and Instrumentation for Astronomy VIII, 99140B (19 July 2016); doi: 10.1117/12.2233472

**SPIE.**

Event: SPIE Astronomical Telescopes + Instrumentation, 2016, Edinburgh, United Kingdom

# Ultra-low Noise TES bolometer Arrays for SAFARI Instrument on SPICA

P. Khosropanah<sup>\*a</sup>, T. Suzuki<sup>b</sup>, M.L. Ridder<sup>a</sup>, R.A. Hijmering<sup>a</sup>, H. Akamatsu<sup>a</sup>, L. Gottardi<sup>a</sup>,  
J. Van der Kuur<sup>a</sup>, J.-R. Gao<sup>a,c</sup>, B.D. Jackson<sup>a</sup>

<sup>a</sup>SRON Netherlands Institute for Space Research, Utrecht, the Netherlands

<sup>b</sup>Graduate School of Science, Nagoya University, Furu-cho Chikusa-ku, Nagoya, 464-8602, Japan

<sup>c</sup>Kavli Institute of NanoScience, Delft University of Technology, Delft, the Netherlands

## ABSTRACT

SRON is developing ultra-low noise Transition Edge Sensors (TESs) based on a superconducting Ti/Au bilayer on a suspended SiN island with SiN legs for the SAFARI instrument aboard the SPICA mission. We successfully fabricated TESs with very narrow (0.5-0.7  $\mu\text{m}$ ) and thin (0.25  $\mu\text{m}$ ) SiN legs on different sizes of SiN islands using deep reactive-ion etching process. The pixel size is  $840 \times 840 \mu\text{m}^2$  and there are variety of designs with and without optical absorbers. For TESs without absorbers, we measured electrical NEPs as low as  $< 1 \times 10^{-19} \text{ W}/\sqrt{\text{Hz}}$  with response time of 0.3 ms and reached the phonon noise limit. Using TESs with absorbers, we quantified the darkness of our setup and confirmed a photon noise level of  $2 \times 10^{-19} \text{ W}/\sqrt{\text{Hz}}$ .

**Keywords:** SPICA, SAFARI, Transition edge sensor, TES arrays, far infrared spectrometer, SiN membrane.

## 1. INTRODUCTION

SPICA (SPace Infrared telescope for Cosmology and Astrophysics) is a future space mission for mid- and far-infrared (IR) astronomy. By having a large (2.5 m) and cooled ( $< 8 \text{ K}$ ) telescope combined with ultra-sensitive IR detectors, SPICA provides an opportunity to make natural background-limited observations over the wavelength range from 17 to 230  $\mu\text{m}$ . One of the instruments aboard SPICA is SAFARI (SpicA FAR-infrared Instrument), which is a grating spectrometer covering the full 34-230  $\mu\text{m}$  wavelength range. SAFARI detectors are transition edge sensor (TES) bolometers for four wavelength bands: S-band for 34-56  $\mu\text{m}$ , M-band for 54-89  $\mu\text{m}$ , L-band for 87-143  $\mu\text{m}$  and LL-band for 140-230  $\mu\text{m}$ . Each band requires a large number of pixels ( $\sim 600$ -2000 pixels) and an extremely high sensitivity (electrical Noise Equivalent Power, NEPEl  $\sim 2 \times 10^{-19} \text{ W}/\sqrt{\text{Hz}}$  at frequencies below  $\sim 100 \text{ Hz}$ ). These requirements impose a great challenge on the detector technology [1].

SRON has been developing ultra-low noise TESs based on a superconducting Ti/Au bilayer on a thin SiN island membrane suspended by narrow and long SiN legs. Fig. 1 (a) shows an SEM picture of the TES array under test and (b) a picture of one of these devices. Three types of devices were designed and fabricated to study the effect of the large SiN island and an absorber on the noise. TES-A has a large SiN island that accommodates a bolometer and an absorber; TES-B has the same size of the island as TES-A with the same bolometer, but without the absorber; TES-C has a tiny island without the absorber, but with the same bolometer as TES-A and -B.

All bolometers are  $50 \times 50 \mu\text{m}^2$  and made of Ti/Au (16/65 nm) bilayer on a 0.25  $\mu\text{m}$  thick suspended SiN island. The absorbers are  $200 \times 200 \mu\text{m}^2$  and made of 8 nm thick tantalum (Ta). The large SiN islands are  $220 \times 280 \mu\text{m}^2$  and the small ones  $70 \times 70 \mu\text{m}^2$ . The SiN legs are about 0.5  $\mu\text{m}$  wide and 350  $\mu\text{m}$  long for large devices and 460  $\mu\text{m}$  for small ones.

Fabrication of TES bolometers includes 14 lithography steps and finishes with a deep reactive-ion etching (DRIE) process that is explained in detail by Ridder et al [2].

\*P.Khosropanah@sron.nl; phone +31 88777 5678; fax +31 88777 5601; sron.nl

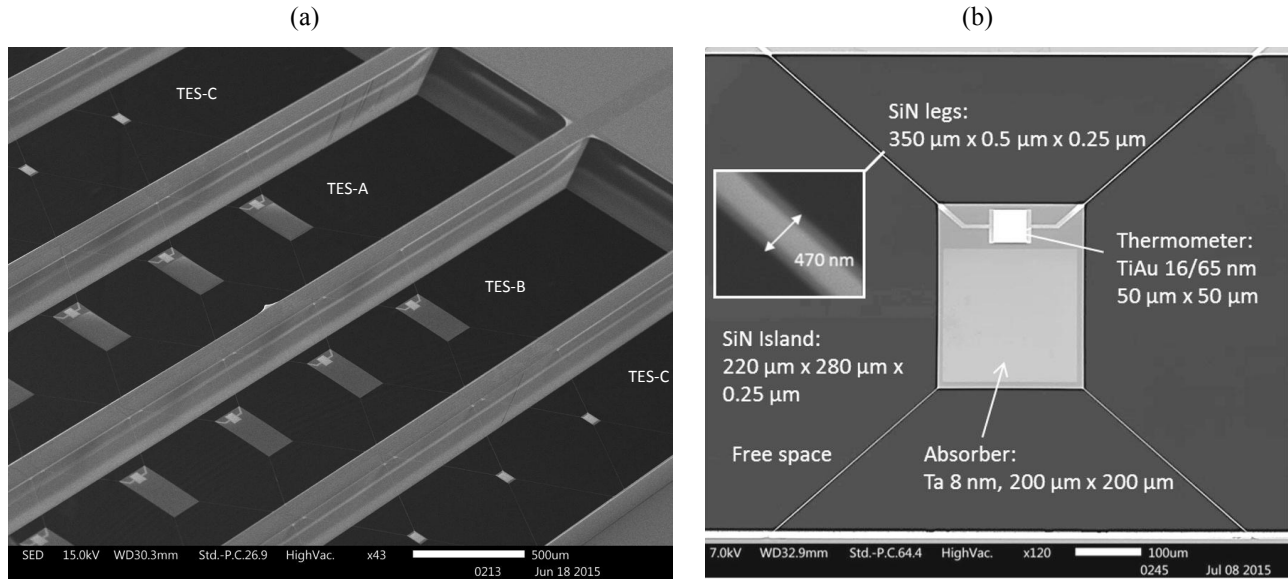


Fig. 1. (a) SEM pictures of the TES array with three types of TES design: a TES with a large SiN island with a Ta optical absorber (TES-A), a TES with a large SiN island without an absorber (TES-B) and a small TES on a small SiN island without an absorber (TES-C). (b) SEM picture of TES-A.

The philosophy behind fabricating these devices was to answer some of the fundamental quotations about the ultra-low TESs: The simplest device (TES-C) is to explore the lowest achievable NEP with this geometry and whether that meets the requirements for SAFARI instrument. A practical TES needs to have a large enough island to accommodate an absorber and TES-B is designed to show how a larger island affects the device performance. The complete device with an absorber (TES-A) is eventually what we need for the instrument.

Previously we reported electrical NEPs as low as  $1.1 \times 10^{-19}$  W/ $\sqrt{\text{Hz}}$  for the TES-C and  $1.5 \times 10^{-19}$  W/ $\sqrt{\text{Hz}}$  for the TES-B devices [3]. The difference between the measured NEPs could be explained by difference in the length of their legs and it was clear that the larger SiN island does not increase the noise. Both values agreed well with the theory that expects the NEP at low frequencies to be dominated by the phonon noise [4]:

$$NEP = \sqrt{4\gamma k_B T_C^2 G} \quad (1)$$

, where  $k_B$  is the Boltzmann's constant,  $T_C$  is the critical temperature of the TES and  $G$  is the thermal conductance between TES and the bath.  $\gamma$  is a number between 0.5 and 1 (in our case about 0.5) that depends on the heat transport mechanism and the critical temperature of the TES ( $T_C$ ) and the bath temperature ( $T_{bath}$ ).

However for TES-A devices the measured NEPs were about  $5-6 \times 10^{-19}$  W/ $\sqrt{\text{Hz}}$ . The observed excess noise is either intrinsic to the device (for example caused by the internal thermal fluctuation noise between the absorber and the TES) or the photon noise due to the stray light, which could only be seen by the devices with absorbers [3]. Since the absorber is very thin and most likely well thermalized with the island, the latter was identified as the source of the extra noise.

To demonstrate a lower noise for a practical device, it is essential to have a darker environment. This paper presents an improved setup that significantly reduces the photon noise level down to  $2 \times 10^{-19}$  W/ $\sqrt{\text{Hz}}$  and reports the measured electrical NEPs of our ultra-low noise TESs in this setup.

## 2. MEASUREMENT SETUP

All measurements were performed in a dilution refrigerator that can cool the TESs down to  $\sim 30$  mK. TESs were characterized under AC bias using our frequency-division multiplexing (FDM) readout system (1–3 MHz) [5]. The frequency separation between neighbor resonators is 100 kHz. The TES array chip and key components of FDM readout were mounted in a low magnetic impurity copper bracket fitted into a niobium shield (see Fig. 2) [6].

The bracket also accommodates a heater, a thermometer and a Helmholtz coil. The heater and thermometer are used to regulate the temperature on the chip mount locally. The coil is for applying a uniform magnetic field on the TES array.

To improve the darkness the bracket was mounted inside a radiation shield that is made of copper and is black-coated inside and outside with 5% carbon loaded Stycast with SiC grains of 1 mm average size to absorb stray light. The whole unit was then covered by yet another copper shield and attached to a 30-mK cold plate (see Fig. 3). All electrical wires were fed through a meander that is potted with Stycast. The unit was vacuum pumped via a 0.5 mm diameter path that is also black-coated inside.

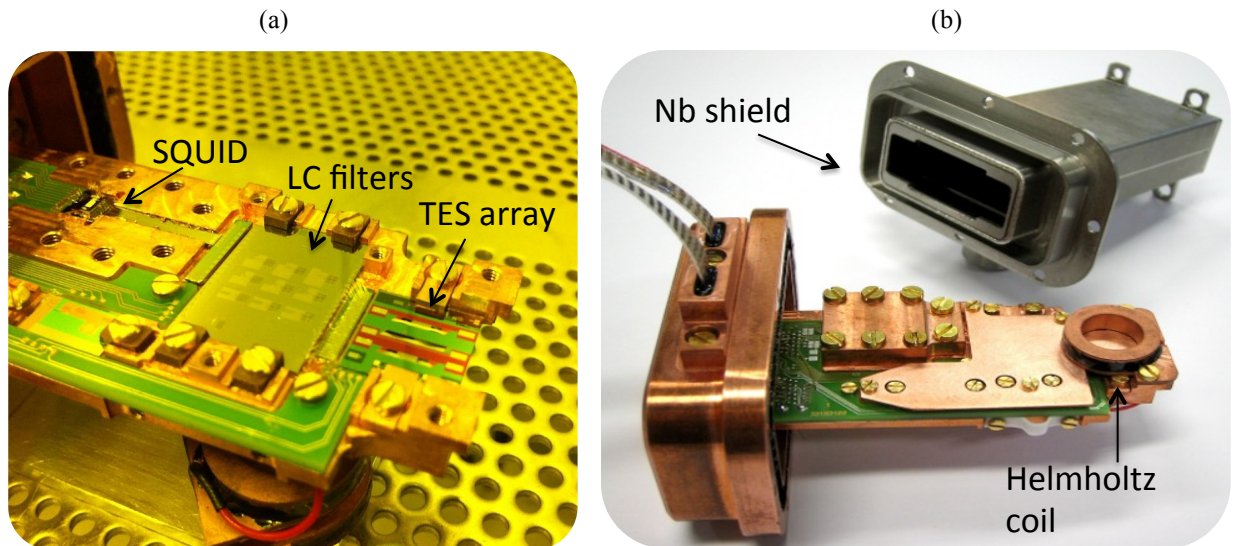


Fig. 2. (a) Picture of the copper bracket that holds the TES array, LC filter chip and the SQUID. (b) The chips were covered by thin copper sheets for protection and a Helmholtz coil was mounted on the top of the TES chip to apply a magnetic field. The whole bracket was then covered by a niobium (Nb) shield.

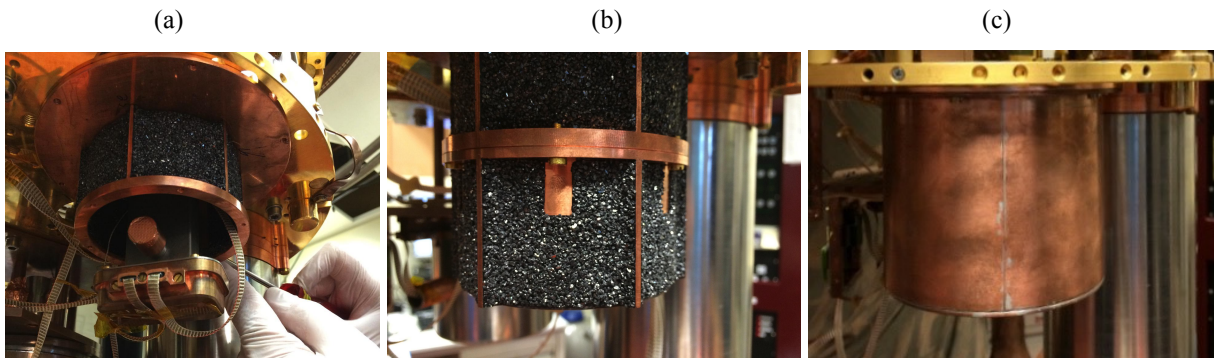


Fig. 3. (a) The bracket was mounted inside a radiation shield and attached to a 30-mK cold plate. The wiring was connected to the feed-through. (b) The radiation shield was closed completely. (c) The whole unit was then covered by a copper shield.

### 3. RESULTS AND DISCUSSIONS

#### 3.1 TES Characterizations

For each TES pixel, we measured both in-phase and quadrature components of TES current, which are related to quasi-particle current that contributes to power dissipation in a TES and Josephson current, respectively [7]; the in-phase component of TES current was only used to characterize the TESs. I-V curves were taken at various bath temperatures and provide TES properties such as saturation power, thermal conductance and responsivity [8]. As for  $R_n$ , it was obtained from measuring the quality factor (Q) when the TES was biased in the normal state. The response speed of the TES was measured by applying a small pulse to the bias line and recording the TES output signal. The pulse amplitude was less than 10% of the bias. The details of these measurements have been reported by Suzuki et al [3].

The critical temperature of these TESs varies between 87-94 mK with normal resistance of 150-160 m $\Omega$ . The thermal conductances are about 60 fW/K for TES-A and -B and about 30 fW/K for TES-C devices. We measure saturation powers of about 1-1.5 fW for TES-A and -B and about 0.8-1.0 fW for TES-C at 60 mK bath temperature. The response time at  $R_{TES}/R_n = 0.3$  in the transition is 0.2 ms for TES-A and -B and about 0.3 ms for TES-C.

#### 3.2 Electrical Noise Equivalent Power

Current noise spectra were measured at 60 mK bath temperature at various bias points in the transition state. At each bias point, the electrical NEP was then calculated from dividing the current density by the responsivity of the TES that is extracted from the calibrated I-V curves. Fig. 4 shows the measured NEPs taken at  $R_{TES}/R_n$  of  $\sim 0.25$ . At frequencies below  $\sim 50$  Hz, TES-C shows the lowest NEP of  $9 \times 10^{-20}$  W/ $\sqrt{\text{Hz}}$  and TES-B shows  $1.1 \times 10^{-19}$  W/ $\sqrt{\text{Hz}}$ . We confirm that these numbers agree with what we reported before within the error bars [3]. At higher frequencies, the measured NEP is higher than the phonon noise for both pixels and shows a bump-like spectrum that is larger for the TES-B, which has a larger island. This feature has also been observed in previous TESs [8-10].

By comparing the NEPs between TESs with and without absorbers, darkness of our setup can be quantified, since it is reasonable to assume that the absorber does not contribute to an additional noise owing to its negligible amount of heat capacity. Although TES-A has quite similar properties to those of TES-B, its NEP is a factor of  $\sim 2$  higher. The excess noise is quantified by quadratic subtraction of the NEP of TES-B from that of TES-A, which results in  $2 \times 10^{-19}$  W/ $\sqrt{\text{Hz}}$  flat spectrum.

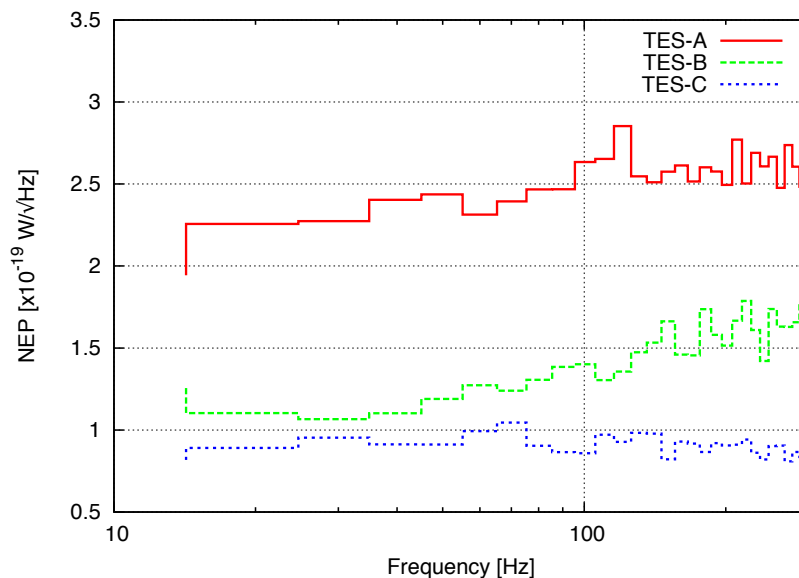


Fig. 4. Measured electrical NEP of TES-A, -B and -C taken at  $R_{TES}/R_n = 0.25$  in the transition.

## 4. SUMMARY

We have made substantial progress towards a generic technology that is capable of delivering the required detectors for SAFARI grating spectrometer. We successfully realized ultra-low-noise TESs with very narrow ( $<0.5\ \mu\text{m}$ ) and thin ( $0.25\ \mu\text{m}$ ) SiN legs and island. For TESs without absorbers, we measured NEPs as low as  $<1\times 10^{-19}\ \text{W}/\sqrt{\text{Hz}}$  with response time of 0.2-0.3 ms and achieved the phonon noise limit at low frequencies below 50 Hz. Similar NEPs were measured after improving the darkness of the setup indicating that the contribution of the photon noise is negligible due to absence of the absorbers. For TESs with absorbers, the NEP was reduced from  $5\text{-}6\times 10^{-19}\ \text{W}/\sqrt{\text{Hz}}$  down to  $2\text{-}2.5\times 10^{-19}\ \text{W}/\sqrt{\text{Hz}}$  after improving the setup. Comparing the NEPs of similar TESs with and without absorbers we quantify the darkness of the setup and confirm photon noise of  $2\times 10^{-19}\ \text{W}/\sqrt{\text{Hz}}$ .

## 5. ACKNOWLEDGEMENTS

The authors are thankful to Damian Audley and Gert de Lange for scientific discussions, and Martijn Schoemans and Kevin Ravensberg for the technical support. European Space Agency (ESA) is acknowledged for supporting this work through TRP program (contract number 22359/09/NL/CP).

## REFERENCES

1. B.D. Jackson, P.A.J. de Korte, J. van der Kuur, P.D. Mauskopf, J. Beyer, M.P. Bruijn, A. Cros, J.-R. Gao, D. Griffin, R. den Hartog, M. Kiviranta, G. de Lange, B.-J. van Leeuwen, C. Macculi, L. Ravera, N. Trappe, H. van Weers, and S. Withington, "The SPICA- SAFARI detector system: TES detector arrays with frequency-division multiplexed SQUID readout," *IEEE Transactions on Terahertz Science and Technology* 2 (99), 1–10 (2011).
2. M.L. Ridder, P. Khosropanah, R.A. Hijmering, T. Suzuki, M.P. Bruijn, H.F.C. Hoevers, J.R. Gao, M.R. Zuiddam, "Fabrication of Low-Noise TES Arrays for the SAFARI Instrument on SPICA," *J. Low. Temp. Phys.* 184, 60–65 (2016).
3. T. Suzuki, P. Khosropanah, M.L. Ridder, R.A. Hijmering, J.R. Gao, H. Akamatsu, L. Gottardi, J. van der Kuur, B.D. Jackson, "Development of Ultra-Low-Noise TES Bolometer Arrays," *J. Low. Temp. Phys.* 184, 52–59 (2016).
4. J. Mather, "Bolometer noise: none-equilibrium theory," *Appl. Opt.* 21, 1125-1129 (1982).
5. R.A. Hijmering, R.H. den Hartog, M.L. Ridder, T. van der Linden, J. van der Kuur, J.R. Gao, B.D. Jackson, "Readout of a 176 pixel FDM system for SAFARI TES arrays," in this SPIE proceedings (2016).
6. L. Gottardi, M. Bruijn, J.-R. Gao, R. den Hartog, R. Hijmering, H. Hoevers, P. Khosropanah, P. de Korte, J. van der Kuur, M. Lindeman, and M. Ridder, "AC bias characterization of low noise bolometers for SAFARI using an open-loop frequency domain SQUID-based multiplexer operating between 1 and 5 MHz," *J. Low. Temp. Phys.* 167, 161-167 (2012).
7. L. Gottardi, A. Kozorezov, H. Akamatsu, J. van der Kuur, M.P. Bruijn, R.H. den Hartog, R. Hijmering, P. Khosropanah, C. Lambert, A.J. van der Linden, M.L. Ridder, T. Suzuki and J.R. Gao, "Josephson effects in an alternating current biased transition edge sensor," *Appl. Phys. Lett.* 105, 162605 (2014).
8. T. Suzuki, P. Khosropanah, R.A. Hijmering, M. Ridder, M. Schoemans, H. Hoevers, J.R. Gao, "Performance of SAFARI Short-Wavelength-Band Transition Edge Sensors (TES) Fabricated by Deep Reactive Ion Etching," *IEEE Trans. THz Sci. Technol.* 4 (2), 171-178 (2014).
9. P. Khosropanah, R.A. Hijmering, M. Ridder, M.A. Lindeman, L. Gottardi, M. Bruijn, J. van der Kuur, P.A. J. de Korte, J.R. Gao, H. Hoevers, "Distributed TES Model for Designing Low Noise Bolometers Approaching SAFARI Instrument Requirements," *J. Low. Temp. Phys.* 167 (3), 188-194 (2012).
10. P. Khosropanah, T. Suzuki, R.A. Hijmering, M.L. Ridder, M.A. Lindeman, J.-R. Gao, H. Hoevers, "Characterization of Low Noise TES Detectors Fabricated by D-RIE Process for SAFARI Short-Wavelength Band," *J. Low. Temp. Phys.* 176 (3), 363-369 (2014).